JOURNAL OF VIROLOGY, Feb. 2008, p. 1284–1293 Vol. 82, No. 3
0022-538X/08/$08.00+0 doi:10.1128/JVI.01164-07

Intracellular Targeting of a Hordeiviral Membrane-Spanning Movement Protein: Sequence Requirements and Involvement of an Unconventional Mechanism▽

Mikhail V. Schepetilnikov,[1,2]† Andrey G. Solovyev,[1,4] Elena N. Gorshkova,[1] Joachim Schiemann,[3] Alexey I. Prokhnevsky,[2] Valerian V. Dolja,[2]* and Sergey Y. Morozov[1]*

A. N. Belozersky Institute of Physico-Chemical Biology, Moscow State University, 119992 Moscow, Russia[1]; Department of Botany and Plant Pathology and Center for Genome Research and Biocomputing, Oregon State University, Corvallis, Oregon 97331[2]; Institute of Plant Virology, Microbiology, and Biosafety, Federal Biological Research Centre for Agriculture and Forestry, Messeweg 11/12, D-38104 Braunschweig, Germany[3]; and Institute of Agricultural Biotechnology, Russian Academy of Agricultural Sciences, Timiryazevskaya 42, 127550 Moscow, Russia[4]

Received 29 May 2007/Accepted 12 November 2007

The membrane-spanning protein TGBp3 is one of the three movement proteins (MPs) of *Poa semilatent virus*. TGBp3 is thought to direct other viral MPs and genomic RNA to peripheral bodies located in close proximity to plasmodesmata. We used the ectopic expression of green fluorescent protein-fused TGBp3 in epidermal cells of *Nicotiana benthamiana* leaves to study the TGBp3 intracellular trafficking pathway. Treatment with inhibitors was used to reveal that the targeting of TGBp3 to plasmodesmata does not require a functional cytoskeleton or secretory system. In addition, the suppression of endoplasmic reticulum-derived vesicle formation by a dominant negative mutant of small GTPase Sar1 had no detectable effect on TGBp3 trafficking to peripheral bodies. Collectively, these results suggested the involvement of an unconventional pathway in the intracellular transport of TGBp3. The determinants of targeting to plasmodesmata were localized to the C-terminal region of TGBp3, including the conserved hydrophilic and terminal membrane-spanning domains.

Cell-to-cell movement of plant viruses includes intracellular trafficking of the genomic nucleoproteins or virions from replication or assembly sites to plasmodesmata, followed by transport through the plasmodesmata. It is believed that most viruses traverse plasmodesmata via microchannels positioned between the plasma membrane and a desmotubule formed by the appressed endoplasmic reticulum (ER) (12, 14). Viral transport normally requires viral movement proteins (MPs) that vary in their provenances, biochemical properties, and even numbers in different viral evolutionary lineages (6, 16, 25, 37, 44). Many plant viral MPs are known to interact with the ER (11, 33, 34, 35, 41, 50, 63), pointing to a link between the endomembrane system and viral movement. Because most, if not all, intracellular motility in eukaryotes involves the cytoskeleton and associated motor proteins, both plant and animal viruses tend to recruit these systems for their own trafficking between cell compartments and neighboring cells (6, 23, 48, 52, 60). Although the exact mechanisms of a plant virus's transport to and through plasmodesmata are by and large unknown, a growing body of evidence suggests a prominent role for the cytoskeleton in this process (6, 24, 30, 33, 47, 51, 55, 66).

Several genera of plant positive-strand RNA viruses of rod-shaped and filamentous morphology possess a conserved set of three MPs encoded by a triple gene block (TGB) (38, 41, 43, 62). The current model of TGB action suggests that the largest TGB protein, TGBp1, possesses ATPase and RNA helicase activities and forms transport-competent ribonucleoprotein complexes with the viral RNA (28, 29, 36), whereas TGBp3 associates with the plasmodesmatal neck region and targets these complexes to plasmodesmata (18, 22, 24, 34, 41, 54, 68, 69). TGBp2, which has the properties of an integral membrane protein, localizes to the ER and intracellular vesicles when expressed alone (26, 40, 56, 59, 70). This protein is redirected by TGBp3 to the plasmodesmatal vicinity and is thought to be required for the TGBp3-mediated localization of TGBp1 to plasmodesmata (19, 68, 69).

Although TGB movement complexes of diverse viruses are homologous, based on their structural properties, they can be subdivided into two classes, potex-like and hordei-like (41). In previous studies, we used green fluorescent protein (GFP)-fused TGBp3 of *Poa semilatent virus* (PSLV; genus *Hordeivirus*) (17, 22, 56, 68), which belongs to a hordei-like class of TGB viruses. Similarly to wild-type PSLV TGBp3, GFP-TGBp3 localizes to the ER-derived compartments and directs TGBp2 and TGBp1 to the cell periphery (22, 68, 69). Moreover, GFP-TGBp3 is capable of functionally substituting for TGBp3 in complementation tests (22; unpublished data). Therefore, GFP-fused PSLV TGBp3 provides an adequate

* Corresponding author. Mailing address for Valerian V. Dolja: Department of Botany and Plant Pathology, Oregon State University, Cordley Hall 2082, Corvallis, OR 97331. Phone: (541) 737-5472. Fax: (541) 737-3573. E-mail: doljav@science.oregonstate.edu. Mailing address for Sergey Y. Morozov: A. N. Belozersky Institute of Physico-Chemical Biology, Moscow State University, Moscow 119992, Russia. Phone: 7 (495) 939-3198. Fax: 7 (495) 939-3181. E-mail: morozov@genebee.msu.su.

† Present address: Institut de Biologie Moléculaire des Plantes, Laboratoire propre du CNRS (UPR 2357) conventionné avec l'Université Louis Pasteur (Strasbourg 1), Strasbourg, France.

▽ Published ahead of print on 21 November 2007.

mechanistic model with which to study the trafficking of a membrane-embedded viral MP.

In this work, we show that the intracellular transport of hordei-like TGBp3 occurs by an unconventional coat protein complex II (COPII)- and cytoskeleton-independent pathway. We also demonstrate that the C-terminal part of TGBp3 that includes a conserved hydrophilic region and a transmembrane domain is both essential and sufficient for the localization of TGBp3 to plasmodesma-associated peripheral bodies.

MATERIALS AND METHODS

Recombinant clones. Recombinant plasmids pRT-GFP-18K, pRT-GFP-18Kmut71, and pRT-GFP-18Kmut62 (56); pCB-Hsp70h-GFP and pCB-GFP-talin (51); and pRT-ST-YFP and pRT-Sar1(T34N) (54) have been described previously. To obtain mutants 18KdN, 18KdA, and 18KdB, the 3′-end-proximal part of the TGBp3 gene was amplified with minus-sense primer Right (56) and one of the following plus-sense primers: 5′-CGCGGATCCATGGGGAATAA TAACCCATATGT, 5′-GAGGGATCCTTTGGTGAACACCCTGTAGA, and 5′-GGGAGGGATCCAATAATCTAGTGTCTAG, respectively. The BamHI/XbaI-digested products were cloned into similarly digested pRT-GFP-18K to replace the wild-type sequence. The mutants mut5Hy, mutK/L, mutK2/L, and mut5Hy were generated by the site-directed mutagenesis of pRT-GFP-18K. To obtain mutant 18KIId4, the 5′-end-proximal part of the TGBp3 gene was amplified with the plus-sense primer Left (56) and the minus-sense primer 5′-CC GCTCTAGATTACTTTAGTAATAGTAAGAATAATAAACC. The BamHI/XbaI-digested product was cloned into similarly digested pRT-GFP-18K to replace the wild-type sequence. For agroinfiltration experiments, the GFP-18K gene was amplified with a pair of primers, 5′-CGTTAATTAATGGTGAGCAA GGGC and 5′-TATAGGCCGGCCCTTAAAGATTATG. The PacI/FseI-digested PCR product was cloned into the binary vector pCB302 (67) to obtain pCB-GFP-18K. To obtain pCB-mRFP-18K, genes of the 18K protein and monomeric red fluorescent protein (mRFP) (Clontech) were amplified with pairs of primers: 5′-TATAGGCCGGCCGCAATGCCTCATC and 5′-TATAGGCGCG CCTTACTTAAAGATTATG and 5′-TCTATTAATTAATGGTGAGCAAGG GCGAG and 5′-TATAGGCCGGCCACTTGTACAGCTC, respectively. The PacI/FseI-digested mRFP and FseI/AscI-digested 18K PCR products were cloned into the binary vector pCB302, which was digested with PacI and AscI. To obtain pRT-18K-GFP, genes of the 18K protein and enhanced GFP (Clontech) were amplified with pairs of primers: 5′-GGATTAATTAATGGCAATGCCTC and 5′-TATAGGCCGGCCCTTAAAGATTATG and 5′-TATAGGCCGGCCT GTGAGCAAGGGC and 5′-TAGGCGCGCCTTACTTGTACAGCTCG, respectively. The PacI/FseI-digested 18K and FseI/AscI-digested enhanced GFP PCR products were cloned into the binary vector pCB302 (67), which was digested with PacI and AscI. For the bombardment experiments, the expression cassette flanked by HindIII sites was cloned from pCB-18K-GFP into pRT103 (58). For visualization of the microtubules, we used the transgenic *Nicotiana benthamiana* line CB13 provided by Karl Oparka (21).

Transient protein expression. Particle bombardment of *N. benthamiana* leaves was performed using the flying disc method with a high-pressure, helium-based PDS-1000 system (Bio-Rad), as described previously (42). For transient protein expression by agroinfiltration, *Agrobacterium tumefaciens* strain GV2260/C58C1 was used. Bacteria carrying pCB302-based vectors were cultured overnight at 28°C with 10 mM 2-*N*-morpholino)ethanesulfonic acid (MES) and 20 mM acetosyringone; resuspended in 10 mM MES (pH 5.85), 10 mM $MgCl_2$, 150 μM acetosyringone to a final optical density at 600 nm from 0.5 to 1.0; incubated for 3 h at room temperature; and infiltrated into the lower leaf surfaces of young (six- to seven-leaf-stage) *N. benthamiana* plants with a needleless syringe. The plants were incubated for 24 h in a growth chamber at 24°C before microscopy was performed.

Drug treatments. Treatments with cytoskeleton-affecting drugs were carried out essentially as described previously (51). Dimethyl sulfoxide (DMSO) stock solutions containing latrunculin B (2 mM; Calbiochem), cytochalasin D (20 mM; ICN), oryzalin (20 mM; ChemService), trifluralin (20 mM; ChemService), phalloidin (5 mM; Calbiochem), taxol (10 mM; Sigma), and brefeldin A (BFA; 10 mg/ml; Sigma) were used for the drug treatment experiments. The drug treatments were done by infiltrating drug solutions diluted 1:1,000 in an agroinfiltration buffer (10 mM MES [pH 5.85], 10 mM $MgCl_2$, 150 μM acetosyringone) into *N. benthamiana* leaves. Equivalent concentrations of DMSO were used in the control experiments.

Confocal laser-scanning microscopy. Cells expressing fusions of fluorescent proteins were imaged on a Zeiss LSM 510 META system with the following combinations of excitation and emission filters, respectively: 488-nm and 508-nm filters for GFP, 513-nm and 527-nm filters for yellow fluorescent protein (YFP), and 558-nm and 583-nm filters for DsRed and mRFP. The software package provided by the manufacturer was used for the three-dimensional reconstructions and image processing.

RESULTS

The trafficking of TGBp3 to peripheral bodies is independent of microtubules and microfilaments. Previous localization studies revealed that the GFP-fused PSLV protein TGBp3 is targeted to discrete peripheral bodies, the ER-derived structures found in close proximity to the plasma membrane (56, 68). Colocalization of peripheral bodies with callose (22) and the protein At-4/1, which is capable of trafficking between cells (49), suggested an association of the peripheral bodies with plasmodesmata. To further investigate this possible association, TGBp3 was coexpressed with two plant virus MPs known to be localized to the plasmodesmata, p30 of *Tobacco mosaic virus* (TMV; genus *Tobamovirus*) (13, 57) and Hsp70h of *Beet yellows virus* (BYV; genus *Closterovirus*) (39, 51). In these experiments, we used agrobacterium-mediated transient coexpression of pairs of proteins tagged with different fluorophores in *Nicotiana benthamiana* leaves. GFP-fused TMV p30 (30K-GFP) was coexpressed with RFP-fused TGBp3 (DsRed-18K [68]), whereas BYV Hsp70h-RFP was coexpressed with GFP-fused TGBp3 (GFP-18K). Independent imaging of the GFP and RFP signals in epidermal cells and the subsequent superposition of images revealed a colocalization of TGBp3 with p30 and Hsp70h (Fig. 1), therefore confirming the plasmodesmatal targeting of TGBp3. Because both TMV p30 (66) and BYV Hsp70h (51) were reported to depend on the cytoskeleton for their trafficking to plasmodesmata, we set out to determine if cytoskeletal motility is involved in PSLV TGBp3 localization to plasmodesmata by use of drugs that specifically disrupt the function of either actin microfilaments or microtubules.

The inhibitors targeting the actin cytoskeleton included latrunculin B and cytochalasin D, which disassemble microfilaments, and phalloidin, which stabilizes microfilaments and prevents their normal dynamics. Analogously, oryzalin and trifluralin were used to depolymerize microtubules, while taxol was used to stabilize microtubules. These expected effects of the cytoskeleton-specific drugs in leaf epidermal cells were confirmed in the control experiments, in which either microfilaments or microtubules were visualized using GFP-talin or GFP-tubulin, respectively (Fig. 2A and B). Moreover, in full agreement with previous work (51), latrunculin B and cytochalasin D, but none of the other inhibitors, interfered with the plasmodesmatal localization of BYV Hsp70h-GFP (Fig. 2D).

Surprisingly, neither microfilament-specific nor microtubule-specific drugs had any detectable effect on the localization of ectopically expressed GFP-18K to plasmodesma-associated peripheral bodies in leaf epidermal cells (Fig. 2C). These results indicated that TGBp3 does not require the cytoskeleton for proper subcellular targeting. It should be emphasized that the drugs were applied twice: 1 day prior to and at the time of agroinfiltration. This approach ensured that the microtubules

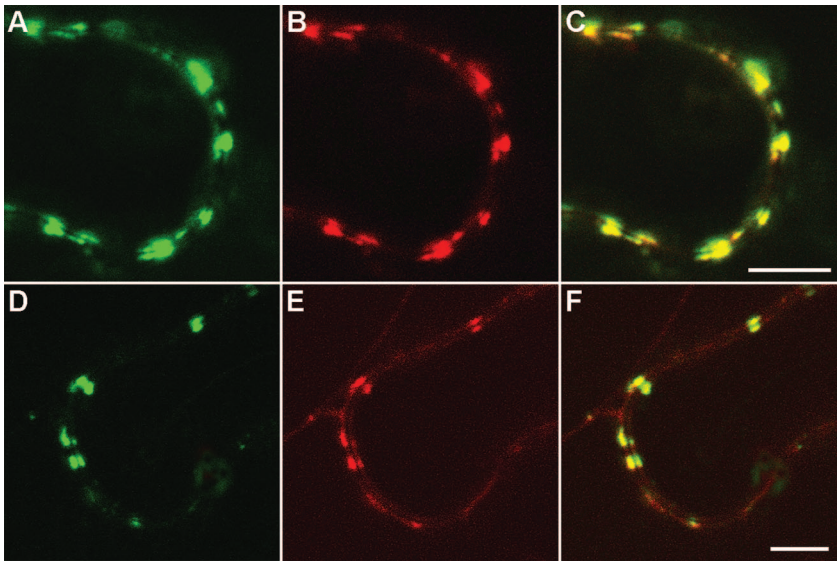

FIG. 1. Confocal laser-scanning microscopy of *N. benthamiana* epidermal cells transiently expressing fluorescent fusion proteins after agroinfiltration. (A to C) Colocalization of 30K-GFP (A) and DsRed-18K (B). (C) Superposition of the images in panels A and B. (D to F) Colocalization of Hsp70h-RFP (E) with GFP-18K (D). (F) Superposition of the images in panels D and E. Scale bars = 5 μm.

or microfilaments were disrupted during the entire period of protein expression and observation.

To test whether the cytoskeleton-independent transport to cell wall-associated sites is a conserved feature of TGBp3 from distinct viruses, we analyzed the effects of the actin cytoskeletal inhibitors on the localization of TGBp3 encoded by *Potato virus X* (PVX). DsRed-18K was coexpressed with GFP-fused PVX TGBp3 (54) by particle bombardment, and the leaves were treated with latrunculin B or oryzalin. Neither of these drugs had any detectable effect on PVX TGBp3 localization (Fig. 3B and C). This result indicates that the dissimilar TGBp3s encoded by hordei-like and potex-like TGBs (41) use the similar actin cytoskeleton-independent pathways of plasmodesmatal targeting.

The conventional protein secretion pathway is not required for TGBp3 targeting. To investigate a potential involvement of the endomembrane secretion system in PSLV TGBp3's localization to peripheral bodies, we used two complementary approaches, (i) the pharmacological inhibition of the Golgi function by BFA (15, 46) and (ii) the dominant negative inhibition of COPII-mediated vesicular trafficking between the ER and the Golgi apparatus (1, 32, 64). It is known that the formation and budding of the COPII vesicles from the ER membranes require a small GTPase, Sar1 (4). The substitution of Asn for Thr at amino acid residue 34 of *Nicotiana tabacum* Sar1 results in a protein restricted to an inactive GDP-bound form; ectopic expression of this Sar1(T34N) mutant blocks COPII-dependent vesicular transport. To monitor the architecture and distribution of Golgi stacks, we used a Golgi body-specific marker, rat sialyl transferase (ST)-YFP, in which the N-terminal signal anchor sequence of ST was fused to YFP (54). As shown previously, ST is transported from the ER to the Golgi body via the COPII pathway (7, 10, 53).

As expected, the ectopic expression of ST-YFP in *N. benthamiana* epidermal cells resulted in its accumulation in the numerous motile bodies corresponding to the Golgi stacks (Fig. 4A and C). Upon BFA treatment, these typical discrete structures were no longer detected in ST-YFP-expressing cells. Instead, ST-YFP was present in a polygonal network corresponding to the cortical ER (Fig. 4B). An analogous effect was observed when Sar1(T34N) was coexpressed with ST-YFP by microprojectile bombardment (Fig. 4D). Such redistribution of ST-YFP in response to either BFA treatment or the dominant negative inhibition of vesicular trafficking by Sar1(T34N) was in exact agreement with previous research (7, 10, 46, 53). We also found that in the cells that coexpressed ST-YFP, Sar1(T34N), and the ER marker m-GFP5-ER (68), the ER-like network was labeled with both Golgi and ER markers, indicating the fusion of Golgi stacks with the ER network (data not shown).

As shown in Fig. 4E to K, the localization of GFP-18K to peripheral bodies was not markedly affected by either BFA treatment or Sar1(T34N) expression. In particular, Fig. 4I to K shows normal peripheral localization of GFP-18K (green) in the cell in which the ST-YFP Golgi marker (false red) is absorbed by the ER due to the expression of Sar1(T34N). Collectively, these observations strongly suggested that the ER-to-Golgi body secretory pathway is not essential for the delivery of PSLV TGBp3 to the cell periphery.

In addition, we examined the effect of the inhibition of the secretory pathway by BFA treatment or Sar1(T34N) expression on the subcellular targeting of TMV 30K-GFP. In both cases, the localization of 30K-GFP remained unaffected (Fig. 4L to N), suggesting that the unconventional transport pathway might be involved in the transport of dissimilar plant virus MPs.

The major determinants of TGBp3 targeting to the cell periphery are present in the C-terminal region. Previously, we found that the insertion disrupting the invariant sequence YQDLN in the central hydrophilic region of TGBp3 and the deletion of the C-terminal transmembrane segment (mutants 18Kmut71 and 18Kmut62, respectively) (Fig. 5A) blocked TGBp3 transport to peripheral bodies (56). These data sug-

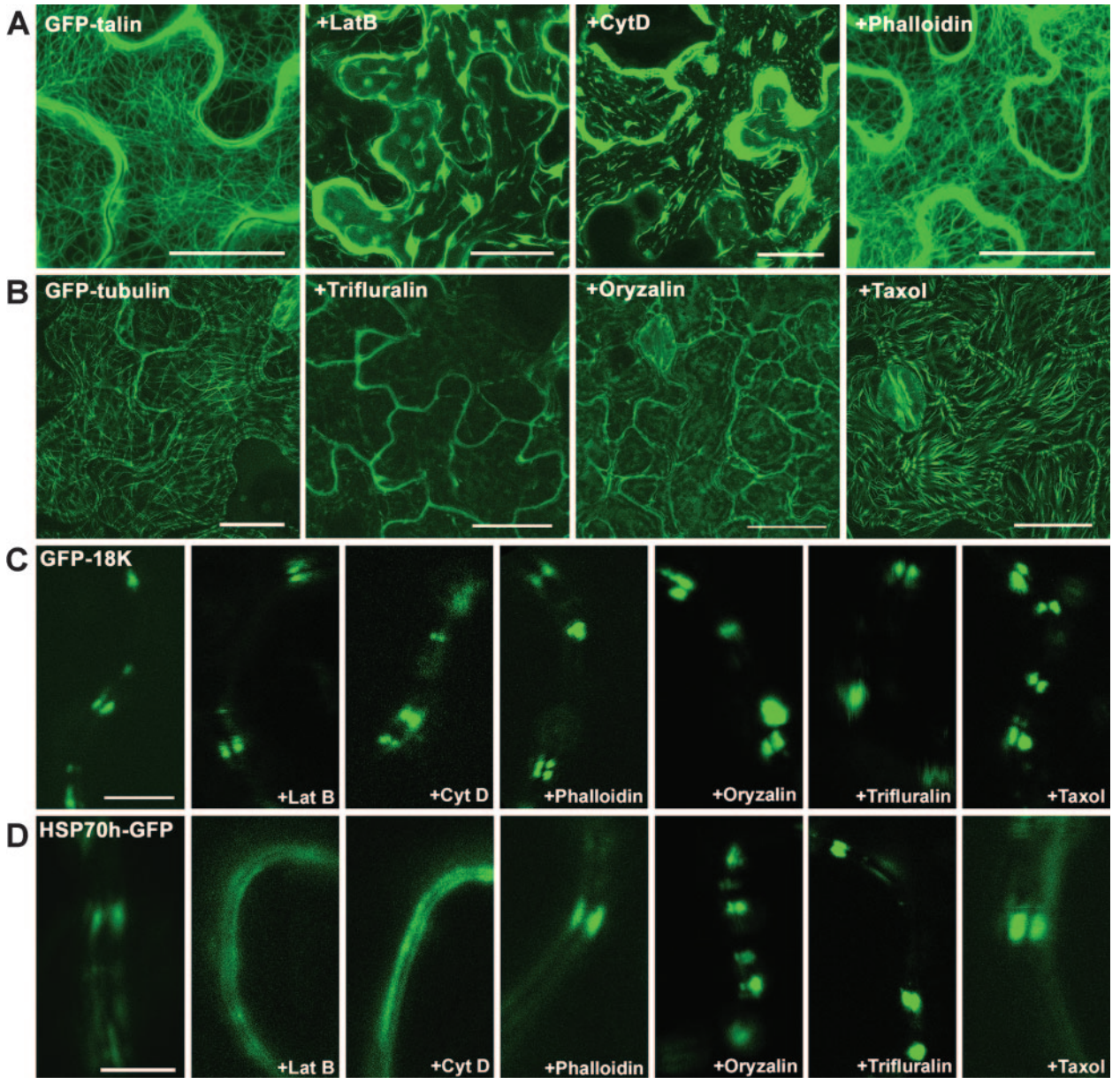

FIG. 2. Effects of the drug treatments on the cytoskeleton and subcellular localization of GFP-18K and Hsp70h-GFP. (A) Microfilaments labeled in the epidermal cells of *N. benthamiana* leaves after the agroinfiltration-mediated expression of GFP-talin. Leaves were treated with DMSO (the control), latrunculin B (LatB), cytochalasin D (Cyt D), or phalloidin. (B) Microtubules in the epidermal cells of *N. benthamiana* leaves labeled with transgenically expressed GFP fused to tubulin. Leaves were treated with DMSO (the control), trifluralin, oryzalin, and taxol. (C and D) High-magnification images of the cell periphery in epidermal cells of *N. benthamiana* leaves that express GFP-18K (C) or Hsp70h-GFP (D) following treatments with various drugs, as indicated on the panels. In the control experiment, *N. benthamiana* leaves were treated with DMSO. The images in panels A and B were constructed by the superposition of a series of confocal optical sections; the images in panels C and D represent single optical sections of the medial cell layer. Scale bars = 20 μm (A and B) and 5 μm (C and D).

gested that the signals responsible for PSLV TGBp3 targeting are localized in the protein's C-terminal region. To further examine the TGBp3 targeting determinants, we generated a series of the N-terminally truncated TGBp3 mutants. In 18KdN, both the N-terminal hydrophilic region and the adjacent hydrophobic sequence were deleted (Fig. 5A). In two other mutants, deletions spanned either the entire protein sequence except for the C-terminal hydrophobic segment (mutant 18KdB) or just the N-terminal hydrophilic region, the first hydrophobic segment, and the most conserved portion of the central hydrophilic sequence (mutant 18KdA) (Fig. 5A). The corresponding GFP-fused mutant proteins were expressed in *N. benthamiana* leaves by particle bombardment. Interestingly, GFP-18KdA and GFP-18KdB were both mislocalized to the ER network, indicating that the C-terminal hydrophobic region alone or in combination with most of the adjacent hydrophilic region was insufficient for protein accumulation in peripheral bodies (Fig. 5C and D). In contrast, GFP-18KdN was

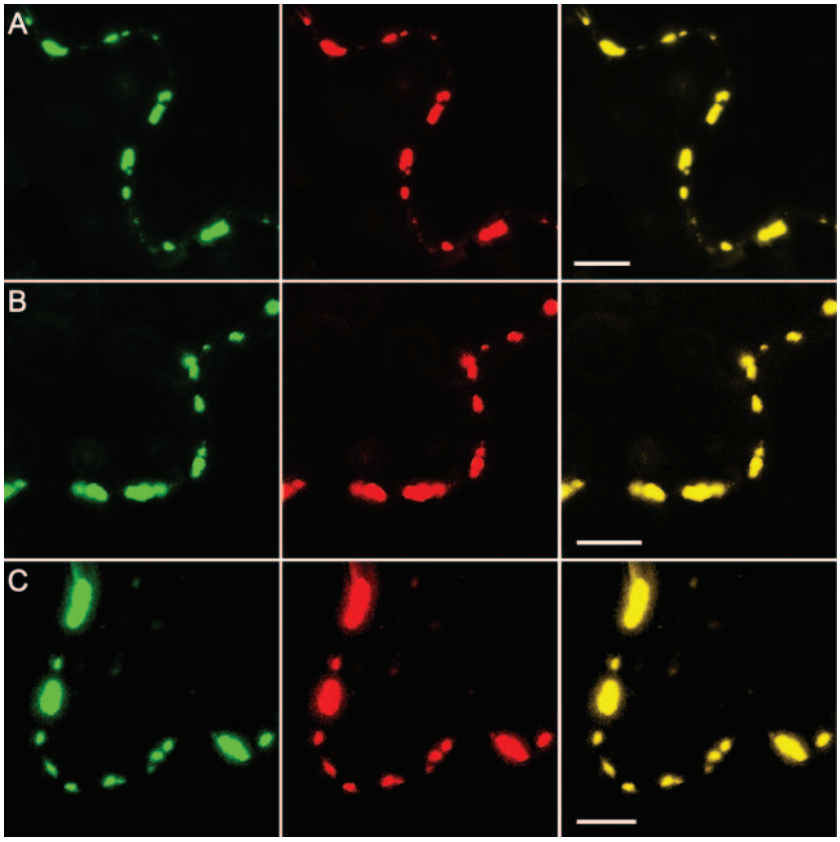

FIG. 3. Effects of the drug treatments on the localization of GFP-fused TGBp3 of PVX (left panels) coexpressed with DsRed-18K (middle panels). The superpositions of the green and red channels are shown in the right panels. Leaves were treated with DMSO (the control) (A), latrunculin B (B), and oryzalin (C). The images represent single optical sections of the medial cell layer. Scale bars = 10 μm.

observed in the peripheral bodies that were indistinguishable from those in cells expressing full-size GFP-18K (Fig. 5B and E).

To gain further understanding of the targeting determinants present in the C-terminal hydrophobic region of PSLV TGBp3, we generated an additional series of TGBp3 mutants. As shown in Fig. 5I, the sequence comparisons revealed that the putative transmembrane C-terminal domain of the hordeiviral TGBp3s varies from 25 to 28 amino acid residues in length and is interrupted by a positively charged residue (Lys in the case of PSLV TGBp3). A similar organization of the C-terminal domain was also found in the TGBp3 of a distantly related *Peanut clump virus* (genus *Pecluvirus*) (Fig. 5I). To determine the potential significance of the conserved Lys residue, it was replaced with Leu to yield the mutant 18KmutK/L (Fig. 5A). A 6-residue-long deletion in the hydrophobic segment upstream of the Lys residue was introduced to obtain 18Kmut5Hy, whereas deletion of the four most-C-terminal hydrophobic residues resulted in 18KmutIId4 (Fig. 5A). In addition, the C-terminal Lys residue was replaced with Leu in the mutant 18KmutK2/L, and the specific sequence downstream of the interrupting Lys was changed to a pseudorandom hydrophobic sequence of Leu/Ile residues in the mutant 18KmutHy (Fig. 5A). Expression of the five corresponding GFP-fused TGBp3 mutants by particle bombardment demonstrated that the subcellular localization of 18KmutK/L, 18KmutK2/L, and 18KmutHy was similar to that of parental GFP-18K (data not shown). As seen in Fig. 5F and G, GFP-18Kmut5Hy and GFP-18KmutIId4 were localized to a granular network dramatically distinct from the peripheral localization of the nonmutant GFP-18K.

The fusion protein 18K-GFP, in which GFP was fused to the C terminus of PSLV TGBp3, was generated to determine if the terminal rather than the internal location of the second hydrophobic domain is essential for the proper targeting of this protein. It was found that 18K-GFP accumulated in the abnormal ER-like network containing numerous irregular inclusions (Fig. 5H).

Collectively, the results of our mutational analysis indicate that the C-terminal part of PSLV TGBp3 that encompasses the central, conserved hydrophilic region and the terminal transmembrane domain determines the localization of TGBp3 to plasmodesma-associated peripheral bodies. In addition, we found that the C-terminal location and the length rather than a specific amino acid sequence of the transmembrane domain are the important determinants of the plasmodesmatal targeting of PSLV TGBp3.

DISCUSSION

Previous work on TGB-mediated viral cell-to-cell movement suggested that the endomembrane-anchored viral movement protein TGBp3 is the key determinant of the intracellular

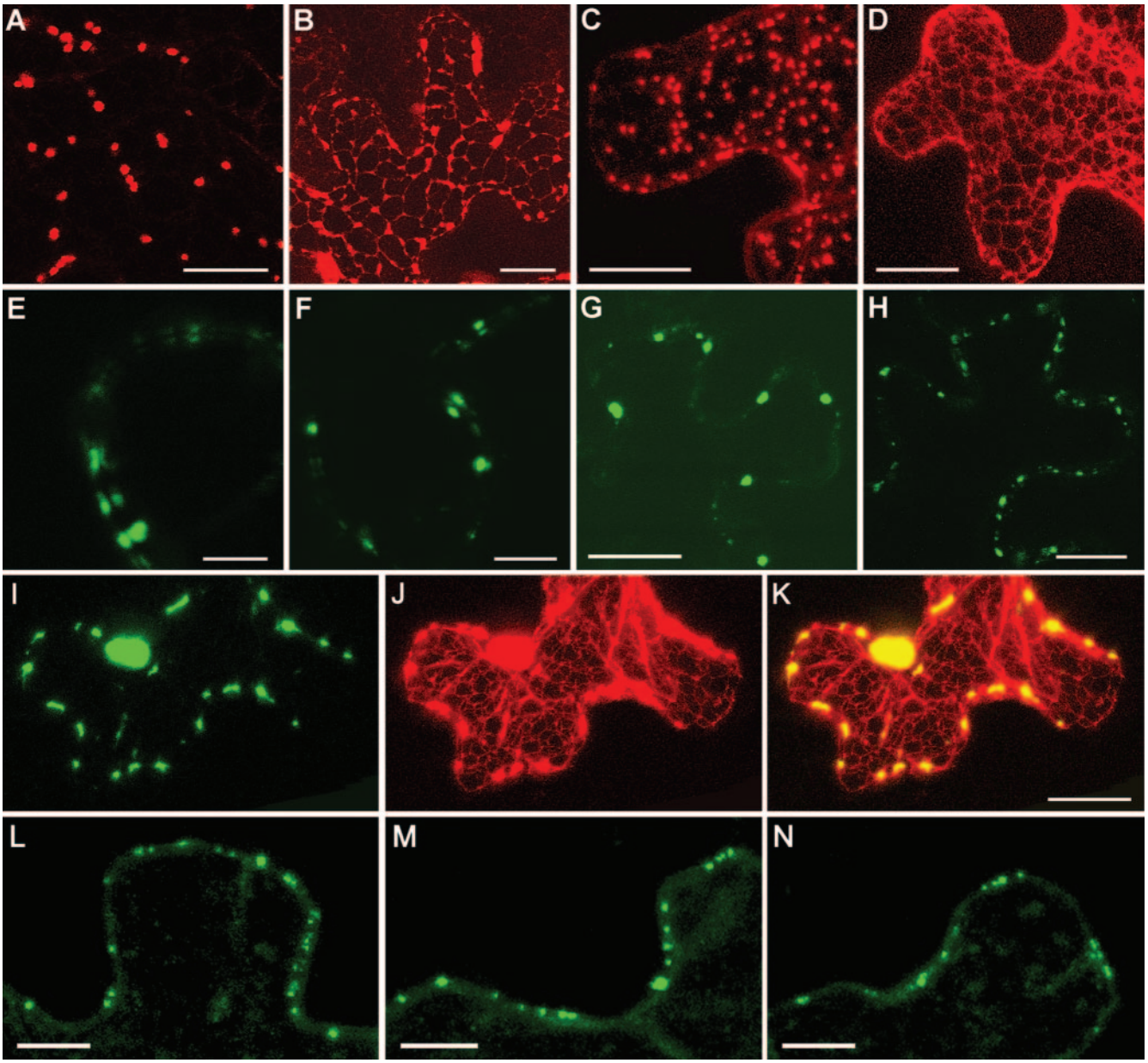

FIG. 4. Influence of BFA treatment and the dominant negative mutant Sar1(T34N) on the subcellular localization of PSLV TGBp3 and TMV MP in *N. benthamiana* leaves revealed by confocal laser-scanning microscopy. (A to D) Ectopic expression of ST-YFP by agroinfiltration (A and B) or by microprojectile bombardment (C and D). (B) ST-YFP-expressing leaves were treated with BFA. (D) ST-YFP was coexpressed with Sar1(T34N). (E to H) Subcellular localization of GFP-18K detected after agroinfiltration (E and F) or microprojectile bombardment (G and H). (F) GFP-18K-expressing leaves were treated with BFA. (H) GFP-18K was coexpressed with Sar1(T34N). (I to K) Coexpression of GFP-18K (I), ST-YFP (J), and Sar1(T34N) by microprojectile bombardment. (K) Superposition of the images in panels A and B. (L to N) Localization of 30K-GFP expressed in *N. benthamiana* leaves by microprojectile bombardment. (M) 30K-GFP-expressing leaves were treated with BFA. (N) 30K-GFP was coexpressed with Sar1(T34N). The images in panels A to D and I to K were constructed by the superposition of a series of confocal optical sections. The other images represent single optical sections of the medial cell layer. Scale bars = 10 μm (E, F, L, M, and N) and 20 μm (the other panels).

transport of a viral genome to plasmodesmata (41, 69). Here we confirm that PSLV TGBp3 colocalizes with TMV p30 and BYV Hsp70h, two unrelated viral proteins that are autonomously targeted to plasmodesmata (Fig. 1) (39, 57). Recent work demonstrated that the proper targeting of Hsp70h requires the actin cytoskeleton (51). In addition, actin microfilaments or microtubules were implicated in the intracellular transport of several other viral MPs (2, 24, 33, 26). Unexpectedly, our analysis demonstrated that the drugs that specifically disassemble or stabilize either microfilaments or microtubules had no observable effect on the targeting of either PSLV or PVX TGBp3 to plasmodesmata (Fig. 2 and 3). These results indicated that the localization of diverse TGBp3 variants is independent of cytoskeletal

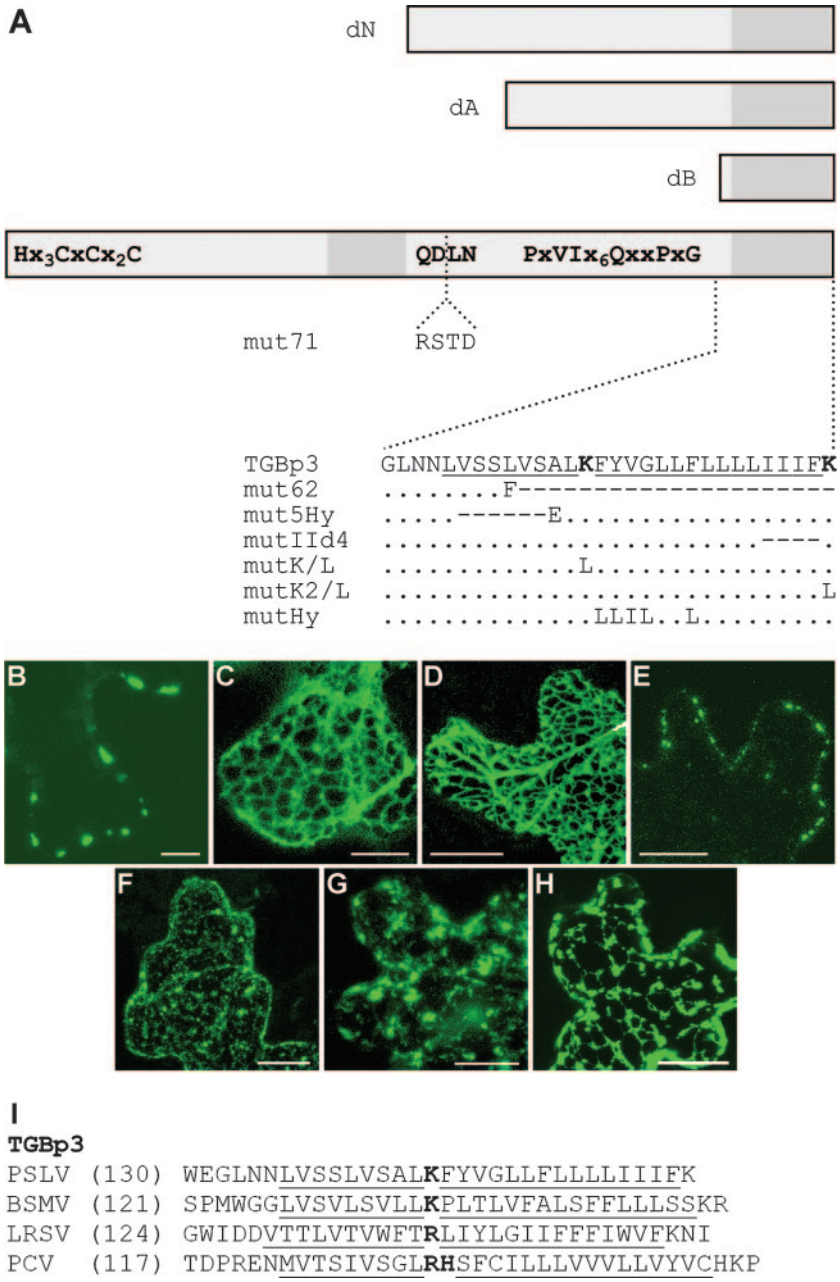

FIG. 5. Construction and subcellular localization of PSLV TGBp3 mutants. (A) Schematic representation of TGBp3 and its mutants. The box represents the TGBp3 sequence. Conserved amino acid motifs are shown. Two hydrophobic sequence segments are shown as dark-gray boxes. The boxes above the protein scheme show the N-terminally truncated mutants dN, dA, and dB. The insertion of four amino acid residues interrupting the conserved tetrapeptide QDLN in mut71 is shown. Below the protein scheme, the sequences of the C-terminal hydrophobic segment and its mutants are shown. In the native sequence, the hydrophobic regions are underlined, and the positively charged Lys residues are shown in bold. For the mutants, amino acid substitutions are shown. The dots indicate identical residues. The dashes indicate deletions. (B to H) Confocal laser-scanning microscopy of *N. benthamiana* epidermal cells transiently expressing fluorescent fusions of PSLV TGBp3 and its mutants after microprojectile bombardment. (B) GFP-18K; (C) GFP-18KdA; (D) GFP-18KdB; (E) GFP-18KdN; (F) GFP-18Kmut5Hy; (G) GFP-18KIId4 18K-GFP; (H) 18K-GFP. All images were constructed by the superposition of a series of confocal optical sections. Scale bars = 20 μm (C, D, and E) and 10 μm (the other panels). (I) Amino acid sequences of the C termini of TGBp3 encoded by three hordeiviruses (*Barley stripe mosaic virus* [BSMV], PSLV, and *Lychnis ringspot virus* [LRSV]) and *Peanut clump virus* (PCV; genus *Pecluvirus*). Hydrophobic sequences are underlined, and interrupting positively charged residues are shown in bold. The numbers in parentheses are the numbers of residues in the protein sequences not shown in the alignment.

motility systems and is therefore mechanistically distinct from that of BYV Hsp70h.

Interestingly, the role of the cytoskeleton in the plasmodesmatal targeting of TMV p30 remains a matter of debate. One line of evidence based primarily on a genetic approach supports microtubule-based motility as the primary means of p30 targeting (9). In contrast, the combination of the pharmaceutical approach and fluorescence recovery after photobleaching

suggested a role for the actin microfilaments but not the microtubules in p30 localization (66). In our hands, neither actin- nor tubulin-depolymerizing drugs affected p30 accumulation in plasmodesmata (51). It seems likely that the apparent discrepancy between the results of these studies is due to different experimental designs. Indeed, the first study examined a correlation between p30 association with microtubules and TMV movement (9), the second investigated the dynamics of p30 accumulation in the plasmodesmata of TMV-infected cells (66), and our study addressed the autonomous targeting of p30 in noninfected cells (51).

Because PSLV TGBp3 is tightly associated with the ER-derived membranes, we were also interested in exploring the possible involvement of vesicular trafficking in TGBp3 delivery to plasmodesmata. As a rule, the intracellular transport of membrane-anchored and secreted proteins involves ER exit in COPII-coated vesicles, which bud from the ER and fuse to the Golgi apparatus (4, 45, 61). We showed that GFP-tagged TGBp3 was able to reach the peripheral bodies in the plasmodesmatal vicinity when the exit of COPII-dependent protein from the ER was suppressed by Sar1(T34N) (Fig. 4), the dominant negative Sar1 mutant which prevents COPII budding complex formation (1, 54, 64). In addition, TGBp3 targeting was insensitive to BFA, which blocks the Golgi body-dependent secretory pathway and induces Golgi body fusion to the ER (Fig. 4). Because the movement of Golgi stacks and transport vesicles in plant cells depends on actin microfilaments (7, 20, 31), the results of our experiments targeting the cytoskeleton and vesicular trafficking are in agreement with each other. Taken together, these data strongly argue against the vesicular model of TGBp3 intracellular transport. We therefore propose that TGBp3 transport occurs via an unconventional pathway that is independent of transport vesicles and the cytoskeleton. In accord with a recent study (66), we found that the vesicular secretion pathway is not required for the plasmodesmatal targeting of TMV p30 (Fig. 4), suggesting that this ER-associated MP may also use an unconventional transport pathway.

We further used mutational analysis to identify the determinants that specify an unusual transport pathway for PSLV TGBp3 to the plasmodesmata. Two sequence elements, the central hydrophilic region containing the conserved pentapeptide YQDLN and the putative C-terminal transmembrane domain, were found to form a composite signal that was both essential and sufficient for targeting PSLV TGBp3 to plasmodesmata. In accord with previous work (10), we also found that the length of the membrane-spanning domain is critical for the proper localization of TGBp3 (Fig. 5). Finally, we showed that this domain should be at the very C terminus of the protein in order to target TGBp3 to the plasmodesmata. It should be emphasized that the mapping of localization determinants to specific regions of TGBp3 supports the functional role of these determinants in their interaction with an endogenous trafficking pathway.

What is the possible mechanism of TGBp3 targeting to plasmodesmata? Since TGBp3 lacks the N-terminal signal peptide, its targeting to membranes is most likely posttranslational, which is rather typical of the tail-anchored proteins (5, 8, 65). One example of such a protein is provided by the yeast integral membrane protein Ist2p, which is sorted to the plasma membrane by translocon-, Golgi body-, and actin microfilament-independent mechanisms (27). It was proposed that Ist2p moves intracellularly by the diffusion or local fusion of the ER and plasma membrane. Another parallel can be drawn from the plant Rop7 protein, a small, membrane-anchored, Ras-related GTPase that requires neither the cytoskeleton nor Golgi stacks for its subcellular targeting (3). By analogy with these plasma membrane-targeted proteins, we hypothesize that TGBp3 traffics to its distinct cellular destination, the plasmodesmatal vicinity, via diffusion in the cytoplasm, possibly by forming a complex with the cell chaperones. The directionality of the TGBp3 transport may be explained by a diffusion-and-retention mechanism, whereby TGBp3 is anchored upon reaching the plasmodesmata. Such anchoring may involve protein-protein interactions mediated by the hydrophilic region adjacent to the C-terminal membrane-spanning domain of TGBp3. The experimental confirmation of this hypothetical model can be obtained by tracing the TGBp3 trafficking pathway using single-molecule imaging techniques. In general, our work highlights the diversity of the cellular trafficking pathways that are recruited by viral proteins to aid their delivery to target cell compartments such as plasmodesmata.

ACKNOWLEDGMENTS

This work was supported in part by a German-Russian intergovernmental program for cooperation in agricultural sciences and by a grant from the Russian Foundation for Basic Research (06-04-49129) to S.Y.M., as well as by a grant from the National Institutes of Health (GM053190) to V.V.D.

REFERENCES

1. **Andreeva, A. V., H. Zheng, C. M. Saint-Jore, M. A. Kutuzov, D. E. Evans, and C. R. Hawes.** 2000. Organization of transport from endoplasmic reticulum to Golgi in higher plants. Biochem. Soc. Trans. **28:**505–512.
2. **Ashby, J., E. Boutant, M. Seemanpillai, A. Sambade, C. Ritzenthaler, and M. Heinlein.** 2006. *Tobacco mosaic virus* movement protein functions as a structural microtubule-associated protein. J. Virol. **80:**8329–8344.
3. **Ashery, U., O. Yizhar, B. Rotblat, and Y. Kloog.** 2006. Nonconventional trafficking of Ras associated with Ras signal organization. Traffic **7:**119–126.
4. **Barlowe, C.** 2003. Signals for COPII-dependent export from the ER: what's the ticket out? Trends Cell Biol. **13:**295–300.
5. **Beilharz, T., B. Egan, P. A. Silver, K. Hofmann, and T. Lithgow.** 2003. Bipartite signals mediate subcellular targeting of tail-anchored membrane proteins in Saccharomyces cerevisiae. J. Biol. Chem. **278:**8219–8223.
6. **Boevink, P., and K. J. Oparka.** 2005. Virus-host interactions during movement processes. Plant Physiol. **138:**1815–1821.
7. **Boevink, P., K. Oparka, S. Santa Cruz, B. Martin, A. Betteridge, and C. Hawes.** 1998. Stacks on tracks: the plant Golgi apparatus traffics on an actin/ER network. Plant J. **15:**441–447.
8. **Borgese, N., S. Colombo, and E. Pedrazzini.** 2003. The tale of tail-anchored proteins: coming from the cytosol and looking for a membrane. J. Cell Biol. **161:**1013–1019.
9. **Boyko, V., Q. Hu, M. Seemanpillai, J. Ashby, and M. Heinlein.** 2007. Validation of microtubule-associated Tobacco mosaic virus RNA movement and involvement of microtubule-aligned particle trafficking. Plant J. **51:**589–603.
10. **Brandizzi, F., E. L. Snapp, A. G. Roberts, J. Lippincott-Schwartz, and C. Hawes.** 2002. Membrane protein transport between the endoplasmic reticulum and the Golgi in tobacco leaves is energy dependent but cytoskeleton independent: evidence from selective photobleaching. Plant Cell **14:**1293–1309.
11. **Brill, L. M., R. S. Nunn, T. W. Kahn, M. Yeager, and R. N. Beachy.** 2000. Recombinant tobacco mosaic virus movement protein is an RNA-binding, alpha-helical membrane protein. Proc. Natl. Acad. Sci. USA **97:**7112–7117.
12. **Citovsky, V., and P. Zambryski.** 1993. Transport of nucleic acids through membrane channels: snaking through small holes. Annu. Rev. Microbiol. **47:**167–197.
13. **Ding, B., J. S. Haudenshield, R. J. Hull, S. Wolf, R. N. Beachy, and W. J. Lucas.** 1992. Secondary plasmodesmata are specific sites of localization of the tobacco mosaic virus movement protein in transgenic tobacco plants. Plant Cell **4:**915–928.
14. **Ding, B.** 1998. Intercellular protein trafficking through plasmodesmata. Plant Mol. Biol. **38:**279–310.
15. **Dinter, A., and E. G. Berger.** 1998. Golgi-disturbing agents. Histochem. Cell Biol. **109:**571–590.

16. **Dolja, V. V., J. F. Kreuze, and J. P. Valkonen.** 2006. Comparative and functional genomics of closteroviruses. Virus Res. **117:**38–51.
17. **Donald, R. G. K., I. T. D. Petty, H. Zhou, and A. O. Jackson.** 1996. Properties of genes influencing barley stripe mosaic virus movement phenotypes, p. 135–147. *In* Fifth International Symposium on Biotechnology and Plant Protection: Viral Pathogenesis and Disease Resistance. World Scientific Publishing, Singapore.
18. **Erhardt, M., M. Morant, C. Ritzenthaler, C. Stussi-Garaud, H. Guilley, K. Richards, G. Jonard, S. Bouzoubaa, and D. Gilmer.** 2000. P42 movement protein of Beet necrotic yellow vein virus is targeted by the movement proteins P13 and P15 to punctate bodies associated with plasmodesmata. Mol. Plant-Microbe Interact. **13:**520–528.
19. **Erhardt, M., G. Vetter, D. Gilmer, S. Bouzoubaa, K. Richards, G. Jonard, and H. Guilley.** 2005. Subcellular localization of the Triple Gene Block movement proteins of Beet necrotic yellow vein virus by electron microscopy. Virology **340:**155–166.
20. **Geldner, N., J. Friml, Y. D. Stierhof, G. Jurgens, and K. Palme.** 2001. Auxin transport inhibitors block PIN1 cycling and vesicle trafficking. Nature **413:** 425–428.
21. **Gillespie, T., P. Boevink, S. Haupt, A. G. Roberts, R. Toth, T. Valentine, S. Chapman, and K. J. Oparka.** 2002. Functional analysis of a DNA-shuffled movement protein reveals that microtubules are dispensable for the cell-to-cell movement of tobacco mosaic virus. Plant Cell **14:**1207–1222.
22. **Gorshkova, E. N., T. N. Erokhina, T. A. Stroganova, N. E. Yelina, A. A. Zamyatnin, Jr., N. O. Kalinina, J. Schiemann, A. G. Solovyev, and S. Y. Morozov.** 2003. Immunodetection and fluorescent microscopy of transgenically expressed hordeivirus TGBp3 movement protein reveals its association with endoplasmic reticulum elements in close proximity to plasmodesmata. J. Gen. Virol. **84:**985–994.
23. **Greber, U. F., and M. Way.** 2006. A superhighway to virus infection. Cell **124:**741–754.
24. **Haupt, S., G. H. Cowan, A. Ziegler, A. G. Roberts, K. J. Oparka, and L. Torrance.** 2005. Two plant-viral movement proteins traffic in the endocytic recycling pathway. Plant Cell **17:**164–181.
25. **Heinlein, M., and B. L. Epel.** 2004. Macromolecular transport and signaling through plasmodesmata. Int. Rev. Cytol. **235:**93–164.
26. **Ju, H. J., T. D. Samuels, Y. S. Wang, E. Blancaflor, M. Payton, R. Mitra, K. Krishnamurthy, R. S. Nelson, and J. Verchot-Lubicz.** 2005. The potato virus X TGBp2 movement protein associates with endoplasmic reticulum-derived vesicles during virus infection. Plant Physiol. **138:**1877–1895.
27. **Juschke, C., D. Ferring, R. P. Jansen, and M. Seedorf.** 2004. A novel transport pathway for a yeast plasma membrane protein encoded by a localized mRNA. Curr. Biol. **14:**406–411.
28. **Kalinina, N. O., D. A. Rakitina, N. E. Yelina, A. A. Zamyatnin, Jr., T. A. Stroganova, D. V. Klinov, V. V. Prokhorov, S. V. Ustinova, B. K. Chernov, J. Schiemann, A. G. Solovyev, and S. Y. Morozov.** 2001. RNA-binding properties of the 63 kDa protein encoded by the triple gene block of poa semilatent hordeivirus. J. Gen. Virol. **82:**2569–2578.
29. **Kalinina, N. O., D. V. Rakitina, A. G. Solovyev, J. Schiemann, and S. Y. Morozov.** 2002. RNA helicase activity of the plant virus movement proteins encoded by the first gene of the triple gene block. Virology **296:**321–329.
30. **Kawakami, S., Y. Watanabe, and R. N. Beachy.** 2004. Tobacco mosaic virus infection spreads cell to cell as intact replication complexes. Proc. Natl. Acad. Sci. USA **101:**6291–6296.
31. **Kost, B., J. Mathur, and N. H. Chua.** 1999. Cytoskeleton in plant development. Curr. Opin. Plant Biol. **2:**462–470.
32. **Kuge, O., C. Dascher, L. Orci, T. Rowe, M. Amherdt, H. Plutner, M. Ravazzola, G. Tanigawa, J. E. Rothman, and W. E. Balch.** 1994. Sar1 promotes vesicle budding from the endoplasmic reticulum but not Golgi compartments. J. Cell Biol. **125:**51–65.
33. **Laporte, C., G. Vetter, A. M. Loudes, D. G. Robinson, S. Hillmer, C. Stussi-Garaud, and C. Ritzenthaler.** 2003. Involvement of the secretory pathway and the cytoskeleton in intracellular targeting and tubule assembly of Grapevine fanleaf virus movement protein in tobacco BY-2 cells. Plant Cell **15:** 2058–2075.
34. **Lawrence, D. M., and A. O. Jackson.** 2001. Interactions of the TGB1 protein during cell-to-cell movement of *Barley stripe mosaic virus*. J. Virol. **75:**8712–8723.
35. **Lazarowitz, S. G., and R. N. Beachy.** 1999. Viral movement proteins as probes for intracellular and intercellular trafficking in plants. Plant Cell **11:**535–548.
36. **Leshchiner, A. D., A. G. Solovyev, S. Y. Morozov, and N. O. Kalinina.** 2006. A minimal region in the NTPase/helicase domain of the TGBp1 plant virus movement protein is responsible for ATPase activity and cooperative RNA binding. J. Gen. Virol. **87:**3087–3095.
37. **Lucas, W. J.** 2006. Plant viral movement proteins: agents for cell-to-cell trafficking of viral genomes. Virology **344:**169–184.
38. **Martelli, G. P., M. J. Adams, J. F. Kreuze, and V. V. Dolja.** 2007. Family Flexiviridae: a case study in virion and genome plasticity. Annu. Rev. Phytopathol. **45:**73–100.
39. **Medina, V., V. V. Peremyslov, Y. Hagiwara, and V. V. Dolja.** 1999. Subcellular localization of the HSP70-homolog encoded by beet yellows closterovirus. Virology **260:**173–181.
40. **Mitra, R., K. Krishnamurthy, E. Blancaflor, M. Payton, R. S. Nelson, and J. Verchot-Lubicz.** 2003. The potato virus X TGBp2 protein association with the endoplasmic reticulum plays a role in but is not sufficient for viral cell-to-cell movement. Virology **312:**35–48.
41. **Morozov, S. Y., and A. G. Solovyev.** 2003. Triple gene block: modular design of a multifunctional machine for plant virus movement. J. Gen. Virol. **84:** 1351–1366.
42. **Morozov, S. Y., O. N. Fedorkin, G. Jüttner, J. Schiemann, D. C. Baulcombe, and J. G. Atabekov.** 1997. Complementation of a potato virus X mutant mediated by bombardment of plant tissues with cloned viral movement protein genes. J. Gen. Virol. **78:**2077–2083.
43. **Morozov, S. Y., V. V. Dolja, and J. G. Atabekov.** 1989. Probable reassortment of genomic elements among elongated RNA-containing plant viruses. J. Mol. Evol. **29:**52–62.
44. **Mushegian, A. R., and E. V. Koonin.** 1993. Cell-to-cell movement of plant viruses. Insights from amino acid sequence comparisons of movement proteins and from analogies with cellular transport systems. Arch. Virol. **133:** 239–257.
45. **Nebenführ, A.** 2002. Vesicle traffic in the endomembrane system: a tale of COPs, Rabs and SNAREs. Curr. Opin. Plant Biol. **5:**507–512.
46. **Nebenführ, A., C. Ritzenthaler, and D. G. Robinson.** 2002. Brefeldin A: deciphering an enigmatic inhibitor of secretion. Plant Physiol. **130:**1102–1108.
47. **Nelson, R. S., and V. Citovsky.** 2005. Plant viruses. Invaders of cells and pirates of cellular pathways. Plant Physiol. **138:**1809–1814.
48. **Oparka, K. J.** 2004. Getting the message across: how do plant cells exchange macromolecular complexes? Trends Plant Sci. **9:**33–41.
49. **Paape, M., A. G. Solovyev, T. N. Erokhina, E. A. Minina, M. V. Schepetilnikov, D. E. Lesemann, J. Schiemann, S. Y. Morozov, and J. W. Kellmann.** 2006. At-4/1, an interactor of the Tomato spotted wilt virus movement protein, belongs to a new family of plant proteins capable of directed intra- and intercellular trafficking. Mol. Plant-Microbe Interact. **19:**874–883.
50. **Peremyslov, V. V., Y.-W. Pan, and V. V. Dolja.** 2004. Movement protein of a closterovirus is a type III integral transmembrane protein localized to the endoplasmic reticulum. J. Virol. **78:**3704–3709.
51. **Prokhnevsky, A. I., V. V. Peremyslov, and V. V. Dolja.** 2005. Actin cytoskeleton is involved in targeting of a viral Hsp70 homolog to the cell periphery. J. Virol. **79:**14421–14428.
52. **Radtke, K., K. Dohner, and B. Sodeik.** 2006. Viral interactions with the cytoskeleton: a hitchhiker's guide to the cell. Cell. Microbiol. **8:**387–400.
53. **Saint-Jore, C. M., J. Evins, H. Batoko, F. Brandizzi, I. Moore, and C. Hawes.** 2002. Redistribution of membrane proteins between the Golgi apparatus and endoplasmic reticulum in plants is reversible and not dependent on cytoskeletal networks. Plant J. **29:**661–678.
54. **Schepetilnikov, M. V., U. Manske, A. G. Solovyev, A. A. Zamyatnin, Jr., J. Schiemann, and S. Y. Morozov.** 2005. The hydrophobic segment of Potato virus X TGBp3 is a major determinant of the protein intracellular trafficking. J. Gen. Virol. **86:**2379–2391.
55. **Seemanpillai, M., R. Elamawi, C. Ritzenthaler, and M. Heinlein.** 2006. Challenging the role of microtubules in *Tobacco mosaic virus* movement by drug treatments is disputable. J. Virol. **80:**6712–6715.
56. **Solovyev, A. G., T. A. Stroganova, A. A. Zamyatnin, Jr., O. N. Fedorkin, J. Schiemann, and S. Y. Morozov.** 2000. Subcellular sorting of small membrane-associated triple gene block proteins: TGBp3-assisted targeting of TGBp2. Virology **269:**113–127.
57. **Tomenius, K., D. Clapham, and T. Meshi.** 1987. Localization by immunogold cytochemistry of the virus coded 30 K protein in plasmodesmata of leaves infected with tobacco mosaic virus. Virology **160:**363–371.
58. **Töpfer, R., V. Matzeit, B. Gronenborn, J. Schell, and H.-H. Steinbiss.** 1987. A set of plant expression vectors for transcriptional and translational fusions. Nucleic Acids Res. **15:**5890.
59. **Torrance, L., G. H. Cowan, T. Gillespie, A. Ziegler, and C. Lacomme.** 2006. Barley stripe mosaic virus-encoded proteins triple-gene block 2 and γb localize to chloroplasts in virus-infected monocot and dicot plants, revealing hitherto-unknown roles in virus replication. J. Gen. Virol. **87:**2403–2411.
60. **Tzfira, T., Y. Rhee, M. H. Chen, T. Kunik, and V. Citovsky.** 2000. Nucleic acid transport in plant-microbe interactions: the molecules that walk through the walls. Annu. Rev. Microbiol. **54:**187–219.
61. **van Vliet, C., E. C. Thomas, A. Merino-Trigo, R. D. Teasdale, and P. A. Gleeson.** 2003. Intracellular sorting and transport of proteins. Prog. Biophys. Mol. Biol. **83:**1–45.
62. **Verchot-Lubicz, J.** 2005. A new cell-to-cell transport model for Potexviruses. Mol. Plant-Microbe Interact. **18:**283–290.
63. **Vilar, M., A. Sauri, M. Monne, J. F. Marcos, G. von Heijne, E. Perez-Paya, and I. Mingarro.** 2002. Insertion and topology of a plant viral movement protein in the endoplasmic reticulum membrane. J. Biol. Chem. **277:**23447–23452.
64. **Ward, T. H., R. S. Polischchuk, S. Caplan, K. Hirschberg, and J. Lippincott-Schwartz.** 2001. Maintenance of Golgi structure and function depends on the integrity of ER export. J. Cell Biol. **155:**557–570.

65. **Wattenberg, B., and T. Lithgow.** 2001. Targeting of C-terminal (tail)-anchored proteins: understanding how cytoplasmic activities are anchored to intracellular membranes. Traffic **2:**66–71.
66. **Wright, K. M., N. T. Wood, A. G. Roberts, S. Chapman, P. Boevink, K. M. Mackenzie, and K. J. Oparka.** 2007. Targeting of TMV movement protein to plasmodesmata requires the actin/ER network: evidence from FRAP. Traffic **8:**21–31.
67. **Xiang, C., P. Han, I. Lutziger, K. Wang, and D. J. Oliver.** 1999. A mini binary vector series for plant transformation. Plant Mol. Biol. **40:**711–717.
68. **Zamyatnin, A. A., Jr., A. G. Solovyev, A. A. Sablina, A. A. Agranovsky, L. Katul, H. J. Vetten, J. Schiemann, A. E. Hinkkanen, K. Lehto, and S. Y. Morozov.** 2002. Dual-colour imaging of membrane protein targeting directed by poa semilatent virus movement protein TGBp3 in plant and mammalian cells. J. Gen. Virol. **83:**651–662.
69. **Zamyatnin, A. A., Jr., A. G. Solovyev, E. I. Savenkov, A. Germundsson, M. Sandgren, J. P. Valkonen, and S. Y. Morozov.** 2004. Transient coexpression of individual genes encoded by the triple gene block of potato mop-top virus reveals requirements for TGBp1 trafficking. Mol. Plant-Microbe Interact. **17:**921–930.
70. **Zamyatnin, A. A., Jr., A. G. Solovyev, P. V. Bozhkov, J. P. Valkonen, S. Y. Morozov, and E. I. Savenkov.** 2006. Assessment of the integral membrane protein topology in living cells. Plant J. **46:**145–154.